Title

Second Guessing in Perceptual Decision-Making.

Journal

The Journal of neuroscience : the official journal of the Society for Neuroscience, 40(26)

ISSN

0270-6474

Authors

McLean, Charlotte S
Ouyang, Bowen
Ditterich, Jochen

Publication Date

2020-06-01

DOI

10.1523/jneurosci.2787-19.2020

Peer reviewed

Title: **Second guessing in perceptual decision-making**

Abbreviated title: Second guessing in perceptual decision-making

Authors: **Charlotte S. McLean[1,2], Bowen Ouyang[1,2] and Jochen Ditterich[1,3]**

[1]Center for Neuroscience and Dept. of Neurobiology, Physiology & Behavior, University of California, Davis, Davis, CA 95618

[2]These authors have contributed equally to this work.

[3]Corresponding author: jditterich@ucdavis.edu

Number of pages: 44

Number of figures: 8

Number of tables: 2

Number of multimedia: 0

Number of 3D models: 0

Number of words in abstract: 138

Number of words in introduction: 623

Number of words in discussion: 1,499

Conflict of interest statement: The authors declare no competing financial interests.

Acknowledgments: This study was supported by NSF grant 1156601.

Charlotte McLean is currently affiliated with the University of Texas Southwestern Medical Center.

ABSTRACT

Human subjects of both sexes were asked to make a perceptual decision between multiple directions of visual motion. In addition to reporting a primary choice, they also had to report a second guess, indicating which of the remaining options they would rather bet on, assuming that they got their primary choice wrong. The second guess was clearly informed by the amounts of sensory evidence that were provided for the different options. A single computational integration-to-threshold model, based on the assumption that the second guess is determined by the rank ordering of accumulated evidence at or shortly after the time of the decision, was able to explain the distribution of primary choices, associated response times, and the distribution of second guesses. This suggests that the decisionmaker has access to how well supported unchosen options are by the sensory evidence.

SIGNIFICANCE STATEMENT

Perceptual decisions require conversion of sensory evidence into a discrete choice. Computational models based on the accumulation of evidence to a decision threshold can explain the distribution of choices and associated decision times. Subjects are also able to report the level of confidence in their decision. Here we show that, when making decisions between more than two alternatives, the decisionmaker can even report a second guess that is clearly informed by the sensory evidence. These second guesses show a distribution that is consistent with subjects having access to how much sensory evidence was accumulated for the unchosen options. The decisionmaker therefore has knowledge about the outcome of the decision process that goes beyond just the choice and an associated confidence.

INTRODUCTION

Perceptual decisions require a decisionmaker to make a discrete choice on the basis of sensory information. Substantial work has gone into elucidating the mechanisms that allow the inflowing sensory evidence to be converted into a discrete choice. Integration-to-threshold mechanisms are the currently dominant class of models, the Drift Diffusion Model (DDM) being a popular exemplar (Luce, 1986; Ditterich, 2006; Ratcliff and McKoon, 2008; Ditterich, 2010; Forstmann et al., 2016). These models are based on the idea that sensory evidence for each available option is accumulated until the accumulated evidence for one of the options exceeds a decision threshold. They can explain the distribution of choices and associated response times (RTs) for a wide range of decision tasks (Ratcliff and Smith, 2004) and are consistent with decision-related neural activity, both averaged across trials as well as on a single-trial level (Ditterich, 2006; Bollimunta et al., 2012). It is difficult, however, to pinpoint experimentally how much temporal integration is involved in the process (Ditterich, 2006), and the view that single-trial decision-related neural activity is consistent with a diffusion-like process has been challenged (Latimer et al., 2015).

More recently, confidence in a perceptual decision has become the focus of scientific investigation. Some studies suggest that a common mechanism could explain both the outcome of the decision as well as the reported confidence (Kiani and Shadlen, 2009; Kiani et al., 2014), while other reports have focused on dissociations between subjective confidence and objective decision accuracy (see Rahnev and Denison (2018) for a review). When making binary decisions, the choice and the associated confidence fully describe the outcome of the decision process. When making decisions between more than two alternatives, the decisionmaker could also have knowledge about how well the sensory evidence supported the unchosen options.

Here we ask whether human subjects have access to information about the "relative desirability" of the unchosen options when making perceptual decisions between more than two alternatives and, if so, whether one can provide a quantitative explanation for the distribution of reported second guesses. We used a modified version of the 3-alternative forced choice (3AFC) version of the multi-component Random Dot Motion (RDM) direction discrimination task introduced in Niwa and Ditterich (2008). Briefly, the subject watches an RDM stimulus that simultaneously contains coherent motion in three different directions, all separated by 120 deg. The strength of each motion component is chosen randomly. The observer has to determine the strongest motion component and indicate its direction with an eye movement. The choice and the associated RT are recorded. For this study, subjects were instructed to also report a second guess with a second eye movement. We asked the observers to indicate which of the remaining two options they would rather bet on, assuming they got their primary choice wrong. Once both the primary choice and the second guess had been registered, auditory feedback about the accuracy of the primary choice was provided. Subjects did not receive feedback on their second guess. The task is illustrated in Figure 1. Further details regarding the experimental design can be found in Materials and Methods.

Here we demonstrate that the second guess is clearly informed by the sensory evidence and that a single integration-to-threshold model can explain the distribution of primary choices, associated RTs, and the distribution of second guesses. This suggests that the decisionmaker has access to how much sensory evidence had been accumulated for options other than the chosen one at the time when the decision was made. We also consider alternative models and show that the second-best explanation for the data is provided by a model that starts a new decision process between the remaining alternatives when the primary decision is made and reads out the decision variable after a fixed amount of time.

MATERIALS AND METHODS

Experimental Design and Statistical Analyses

Human Subjects

The study was approved by the UC Davis Institutional Review Board. After giving their informed consent, seven UC Davis undergraduate students (4 females, 3 males) with normal or corrected-to-normal vision participated in the experiment. Each of the subjects completed at least five experimental sessions with a minimum of 300 valid decision trials each.

Experimental Setup

The subjects sat in front of a 22" flat-screen CRT video monitor (ViewSonic P225f; viewing distance: 60 cm) with their head on a chin and forehead rest. The visual stimuli were generated by a Macintosh G4 computer running Mac OS 9, MATLAB (The Mathworks, Natick, MA), and the Psychophysics Toolbox (Brainard, 1997; Pelli, 1997) at a frame rate of 75 Hz. The experiment was controlled and the data were collected by an Intel Pentium IV computer running QNX (Ottawa, ON, Canada) and a modified version of REX (Laboratory of Sensorimotor Research, National Eye Institute).

Eye movements were monitored using a monocular IR video eye tracker with chinrest-mounted optics (Series 5000, Applied Science Laboratories, Bedford, MA) operating at 240 Hz. Prior to each experimental session the eye tracker was calibrated using repeated fixation of nine calibration targets with horizontal eccentricities of -10, 0, and +10 deg and vertical eccentricities of -7.5, 0, and +7.5 deg.

Experimental Task and Visual Stimulus

The experimental task is illustrated in Fig. 1. Each trial started with the presentation of a central fixation mark (diameter: 0.3 deg). The measured fixation location had to remain within 2.5 deg of the center of the screen throughout the trial (up to the saccadic response). After 250 to 500 ms of stable fixation, three targets (diameter: 0.5 deg) appeared on the screen, all located on a virtual circle around the fixation mark with a radius of 8.0 deg. The target locations were chosen randomly (with equal spacing) at the beginning of an experimental sessions and did not change throughout the session. After another random delay of 250 to 500 ms, a multi-component random-dot pattern was presented at the center of the screen (diameter: 5.0 deg).

In the original version of the stimulus (as used, e.g., in Shadlen and Newsome, 2001; Roitman and Shadlen, 2002; Palmer et al., 2005) a certain fraction of the dots (defined as the coherence of the stimulus) was moving coherently in a particular direction, whereas the remaining dots were flickering randomly. Our multi-component random-dot pattern had up to three coherent motion components embedded. Thus, there were four subpopulations of dots: one was moving coherently in a particular direction θ (aligned with one of the choice targets; fraction of dots defined by the coherence of the first component), another one was moving coherently in the direction $\theta + 120^\circ$ (fraction defined by the coherence of the second component), a third one was moving coherently in the direction $\theta + 240^\circ$ (fraction defined by the coherence of the third component), and the remaining dots were flickering randomly. The stimulus is therefore described by a set of three coherences. Which of the four subpopulations a particular dot belonged to, changed randomly over time. As a consequence, the stimulus is not perceived as an overlay of several transparent layers of motion that could be easily separated, but as a mixture of different motion components. See, e.g., Treue et al. (2000) for a discussion of transparent random-dot motion stimuli. Corresponding pairs of dots, responsible for the

percept of apparent motion, were presented with a temporal separation of 40 ms (3 video frames). The coherently moving dots had a speed of 6 deg/s, the dot density was $16.7 \frac{dots}{\deg^2 \cdot s}$, and each dot was a little filled square with an edge length of 0.1 deg. On each trial, the set of coherences was randomly selected from a list of 51 possible coherence combinations ranging from 0 to 40% each. The full list can be found in Table 1.

The subjects were instructed to identify the direction of the strongest motion component and to make a saccadic eye movement to the associated choice target (aligned with the identified direction of motion). They were allowed to watch the stimulus for as long as they wanted (up to 5 s) and to respond whenever they were ready. The motion stimulus disappeared from the screen as soon as the eye left the central fixation window. Subjects were further instructed to indicate with a second saccadic eye movement to one of the two remaining choice targets, which of the remaining options they would rather bet on as a second guess, assuming they got their first choice wrong. After each trial they received auditory feedback as to whether they had picked the correct target in their primary choice. In case the stimulus did not have one strongest motion component, the computer randomly identified one of the targets as being the correct one. No feedback was given on the second guess.

In order to complete a trial successfully ("valid trial"), the subject had to maintain accurate fixation until the random-dot pattern appeared. Once central fixation was broken, the eye position had to be within 3 deg of one of the three choice targets within 100 ms and had to stay on this target (primary choice) for at least 200 ms. At this point, a neutral sound was played, indicating that the primary choice had been registered, but not providing any information about its accuracy yet. At most 3 s later, the eye position had to be within 3 deg of one of the remaining choice targets and had to stay on this target (second

guess) for at least 200 ms. At this point, auditory feedback was given about the accuracy of the primary choice, which indicated to the subject that the trial had been registered as a valid trial.

Data Analysis

For analyzing the data, we collapsed across different target locations. Thus, we only worked with the 15 unique sets of coherences (eliminating the permutations) and whether the subject picked the target associated with the strongest motion component, the one associated with the intermediate component, or the one associated with the weakest component. We analyzed the pooled data across subjects to have a robust number of trials for each experimental condition. Since we only work with mean RTs in this study, we were not concerned about variability in RT across subjects potentially affecting the shape of RT distributions.

RT was defined as the time between the appearance of the random-dot stimulus and the breaking of central fixation. We did not analyze the timing of the second guess as subjects had to wait for their primary choice to be registered by the computer before they could report their second guess. Thus, the timing of the second guess was largely externally imposed.

Computational Models

Model of the neural representation of the sensory stimulus

The mean response of a population of motion-sensitive neurons to a 3-component random-dot stimulus with coherences c_1 (in the preferred direction of the pool), c_2, and c_3 was modeled to be of the form

175 $$\overline{s_1} = \frac{g \cdot \left[c_1 + k_n \cdot \left(1 - \sum_{i=1}^{3} c_i \right) \right]}{1 + k_s \cdot (c_2 + c_3)}$$

176 where g is the overall gain of the sensory response (relationship between neural activity and motion
177 strength). The two additive terms in the brackets reflect the two linear response components: the first
178 describes the response to the coherent motion in the preferred direction, the second describes the
179 response to the noise dots. The term in parenthesis reflects the proportion of noise dots in the stimulus.
180 k_n is the relative gain of the response to the noise dots compared to the response to an identical
181 fraction of dots moving coherently in the preferred direction. The term in the denominator reflects the
182 divisive normalization. Since the term in the numerator accurately describes the response to a single-
183 component stimulus, only the coherences of motion components with directions other than the
184 preferred one are present in the denominator. For simplicity, we have chosen a linear term, with k_s
185 describing the gain/strength of the divisive normalization (Niwa and Ditterich, 2008).

186 In general, the mean responses of each of the three task-relevant sensory pools can be written as

187 $$\overline{s_j} = \frac{g \cdot \left[c_j + k_n \cdot \left(1 - \sum_{i=1}^{3} c_i \right) \right]}{1 + k_s \cdot \sum_{i \neq j} c_i}$$

188 The variances of the three sensory responses were modeled as

189 $$\sigma_{s_j}^2 = k_v \cdot \overline{s_j}$$

190 We described the outputs of the sensory pools as normal random processes to be able to treat the
191 decision process as a standard diffusion process (based on Brownian motion), which is reasonable if the
192 pools are not too small.

193

194 *Model of the decision process*

195 In principle, we would have to treat the race between the three integrators mathematically as a
196 3-dimensional diffusion process. However, for the 2AFC case, the decision process has often been
197 described as a 1-dimensional diffusion process with two boundaries instead of a 2-dimensional diffusion
198 process. This simplification can be done when one assumes that the two signals that are accumulated by
199 the two integrators are only different in sign, but identical in absolute value. Such a situation would
200 result from all of the contributions that a particular pool of sensory neurons makes to the net evidence
201 signals having the same origin. If we make the same assumption in our model, we can also reduce the
202 dimensionality of the problem. We can write the three evidence signals as

203
$$\begin{aligned} e_1 &= s_1 - \tfrac{1}{2}s_2 - \tfrac{1}{2}s_3 \\ e_2 &= s_2 - \tfrac{1}{2}s_1 - \tfrac{1}{2}s_3 \\ e_3 &= s_3 - \tfrac{1}{2}s_1 - \tfrac{1}{2}s_2 \end{aligned}$$

204 e_3 can be rewritten as

205
$$e_3 = -\left(s_1 - \tfrac{1}{2}s_2 - \tfrac{1}{2}s_3\right) - \left(s_2 - \tfrac{1}{2}s_1 - \tfrac{1}{2}s_3\right) = -e_1 - e_2$$

206 Thus, if e_1 and e_2 are known, e_3 is known. In our model, each of the three evidence signals is integrated
207 over time (see Fig. 2):

208
$$i_j(t) = \int_0^t e_j(\tau)\, d\tau$$

209 Since integration is a linear operation, if i_1 and i_2 are known, i_3 is also known. We can therefore rewrite
210 the decision criterion for choosing the 3rd alternative:

211
$$\begin{aligned} i_3 &> 1 \\ -i_1 - i_2 &> 1 \\ i_2 &< -i_1 - 1 \end{aligned}$$

212 Thus, the third integrator exceeding a value of 1 is equivalent to crossing another linear boundary in the

213 i_1 - i_2 plane (for an illustration see Niwa and Ditterich (2008), Fig. 3C). The diffusion process always starts

214 at (0;0) and stops when one of the three boundaries is crossed: $i_1 = 1$ is the decision boundary for the

215 1st alternative, $i_2 = 1$ is the boundary for the 2nd alternative, and $i_2 = -i_1 - 1$ is the boundary for the 3rd

216 alternative.

217 The 2-dimensional diffusion process is described by a drift vector and a covariance matrix. The drift

218 vector is given by $\begin{bmatrix} \overline{e_1} \\ \overline{e_2} \end{bmatrix}$, the means of the first two evidence signals. Since $\begin{bmatrix} e_1 \\ e_2 \end{bmatrix}$ can be calculated as

219
$$\begin{bmatrix} e_1 \\ e_2 \end{bmatrix} = \begin{bmatrix} 1 & -\frac{1}{2} & -\frac{1}{2} \\ -\frac{1}{2} & 1 & -\frac{1}{2} \end{bmatrix} \cdot \begin{bmatrix} s_1 \\ s_2 \\ s_3 \end{bmatrix}$$

220 $\begin{bmatrix} \overline{e_1} \\ \overline{e_2} \end{bmatrix}$ is given by

221
$$\begin{bmatrix} \overline{e_1} \\ \overline{e_2} \end{bmatrix} = \begin{bmatrix} 1 & -\frac{1}{2} & -\frac{1}{2} \\ -\frac{1}{2} & 1 & -\frac{1}{2} \end{bmatrix} \cdot \begin{bmatrix} \overline{s_1} \\ \overline{s_2} \\ \overline{s_3} \end{bmatrix}$$

222 The covariance matrix Σ can be calculated as

$$\Sigma = \begin{bmatrix} 1 & -\frac{1}{2} & -\frac{1}{2} \\ -\frac{1}{2} & 1 & -\frac{1}{2} \end{bmatrix} \cdot \begin{bmatrix} \sigma_{s_1}^2 & 0 & 0 \\ 0 & \sigma_{s_2}^2 & 0 \\ 0 & 0 & \sigma_{s_3}^2 \end{bmatrix} \cdot \begin{bmatrix} 1 & -\frac{1}{2} \\ -\frac{1}{2} & 1 \\ -\frac{1}{2} & -\frac{1}{2} \end{bmatrix} =$$

$$= \begin{bmatrix} \sigma_{s_1}^2 + \frac{1}{4}\sigma_{s_2}^2 + \frac{1}{4}\sigma_{s_3}^2 & -\frac{1}{2}\sigma_{s_1}^2 - \frac{1}{2}\sigma_{s_2}^2 + \frac{1}{4}\sigma_{s_3}^2 \\ -\frac{1}{2}\sigma_{s_1}^2 - \frac{1}{2}\sigma_{s_2}^2 + \frac{1}{4}\sigma_{s_3}^2 & \frac{1}{4}\sigma_{s_1}^2 + \sigma_{s_2}^2 + \frac{1}{4}\sigma_{s_3}^2 \end{bmatrix} = \quad (223)$$

$$= k_v \cdot \begin{bmatrix} \overline{s_1} + \frac{1}{4}\overline{s_2} + \frac{1}{4}\overline{s_3} & -\frac{1}{2}\overline{s_1} - \frac{1}{2}\overline{s_2} + \frac{1}{4}\overline{s_3} \\ -\frac{1}{2}\overline{s_1} - \frac{1}{2}\overline{s_2} + \frac{1}{4}\overline{s_3} & \frac{1}{4}\overline{s_1} + \overline{s_2} + \frac{1}{4}\overline{s_3} \end{bmatrix}$$

Model of the second choice based on accumulated evidence at or shortly after the time of the first threshold crossing

The integrator crossing the decision threshold first determines the primary choice and the decision time. We propose that the state of the remaining integrators at the time when the winning integrator crosses threshold can be used to determine the second guess. The higher value of the two remaining integrators determines the second choice. For example, if the second integrator crossed the threshold first, the states of the first and the third integrator at this particular time would be compared, and the larger value would determine the second guess. As pointed out above, when working with a 2-dimensional stochastic process, the two dimensions correspond to the states of the first two integrators. The state of the third integrator can be calculated as $i_3 = -i_1 - i_2$.

While the first passage time problem could be solved numerically (see Ditterich, 2006, section B.5 and Niwa and Ditterich, 2008), we also needed the predictions for the distribution of second choices. Therefore, we discretized the 2-dimensional diffusion process (time step: 5 ms) and simulated 50,000 trials per experimental condition. The MATLAB function OU_2D_3B_SIM_SC.M, which has been used for performing the model calculations, is part of the Stochastic Integration Modeling Toolbox (SIMT; written by JD), which can be downloaded from https://www.github.com/peractionlab/StochInt.

To determine whether the second guess might have been informed by sensory evidence that arrived at the decision process after the decision threshold had been crossed, we allowed the integration process to continue for a fixed amount of time after the threshold crossing and then read out and compared the states of the integrators that had not won the race to threshold. The MATLAB function used for this purpose, OU_2D_3B_SIM_SC_ADD_TIME.M, is also part of SIMT. To quantify the deviation between predicted and observed second guesses, we calculated the sum of the squared differences between predicted and observed relative frequencies.

Model of the second choice based on two successive threshold crossings

We also considered a model where the integration process continues after the first threshold crossing, until a second (different) bound is crossed. The first threshold crossing determines the first choice, the second threshold crossing the second choice and the decision time. In contrast to our original model, to give this model more flexibility, the integration of sensory evidence was allowed to be leaky (the time constant of integration was an additional free model parameter), and the bounds were allowed to collapse over time. We used the same logistic function as in Ditterich (2006):

$$A(t) = \frac{1}{1+\exp\left(s\cdot\left(t-d\right)\right)} + \frac{\exp\left(-s\cdot d\right)}{1+\exp\left(-s\cdot d\right)}$$

t is the time into the decision process, and s and d are two additional free model parameters that define the shape (slope) and the position (delay) of the collapsing bound. The MATLAB function OU_2D_3B_TWO_CROSS_SIM.M, which was used for evaluating this model, is also part of SIMT.

Models of the second choice based on two successive decision processes

Another class of models involved starting a new decision process when the first threshold crossing occurred, but only between the two alternatives that did not win the original race to threshold. For example, assuming that i_2 crossed the threshold first, the second process would be set up as

$$e_1' = s_1 - s_3$$
$$e_2' = s_3 - s_1$$

If the integral of the first evidence signal crossed the threshold first, Direction 1 would be reported as the second choice. If the integral of the second evidence signal crossed the threshold first, Direction 3 would be reported as the second choice. Since $e_2' = -e_1'$, this second decision process can be treated as a 1-dimensional drift-diffusion process with two boundaries. The decision time would be the total duration of both decision processes. To give this model more flexibility, we allowed the decision threshold of the second decision process to be lower than the decision threshold of the first decision process. The second decision threshold was an additional free model parameter. The MATLAB function OU_2D_3B_1D_2B_SIM_SC.M, which has been used for evaluating this model, is also part of SIMT.

Finally, we considered a model that also starts a second decision process when the first threshold crossing occurs, but it does not wait for a second threshold crossing. The second decision process unfolds for a fixed amount of time and is then read out. The sign of the current state of the integrated evidence (of the 1D process) determines the second choice. The MATLAB function OU_2D_3B_1D_FIXED_TIME_SIM_SC.M, which was used for evaluating this model, is also part of SIMT.

Model Fit

The model parameters were identified by an optimization procedure based on the mean RTs. A combination of a global pattern search (provided by MATLAB's Global Optimization Toolbox) and a multi-dimensional simplex algorithm (provided by MATLAB's Optimization Toolbox) was used to minimize the sum of the squared differences between the mean RTs in the data and the mean RTs predicted by the model, taking the standard errors of the estimated means into account. We used the mean RTs for each combination of coherences, regardless of choice (15 data points). For the model these were obtained by calculating a weighted sum of the predicted mean RTs for the different choices based on the predicted probabilities of these choices.

RESULTS

We used 11,060 valid decision trials from seven subjects for analysis and modeling. The overall accuracy of the primary choice was 72% (chance level would be 33% for a 3AFC task), which provided us with 7,951 correct trials and 3,109 error trials for further analysis. How the primary choice and the associated RT depended on the presented stimulus was similar to what we had reported in Niwa and Ditterich (2008) and will be presented in the context of a computational model below.

Second guesses in perceptual decision-making are informed by sensory evidence

To test whether subjects are able to make an informed second guess, we analyzed the error trials and quantified how often subjects reported what would have been the correct choice as their second guess. If subjects just guessed randomly, this should not deviate significantly from chance (50%). The correct option, however, was reported as the second guess in 63% of the error trials, which is highly significantly

above chance ($p < 10^{-6}$; binomial test). This indicates that the second guess was clearly informed by the sensory evidence provided by the motion stimulus.

A computational model that can explain primary choices and associated RTs

To gain more insight into what information the second guesses were based on, we resorted to computational modeling. In Niwa and Ditterich (2008) we presented an integration-to-threshold model that was able to explain the distribution of choices in the 3-choice multi-component RDM direction discrimination task as well as the associated RTs. Briefly, in a stochastic process, we modeled three pools of motion-sensitive neurons (for each of the possible directions). Each of these pools had a strong linear response to coherent motion in its preferred direction, a weak linear response to the randomly moving dots in the stimulus, and divisive normalization based on how much coherent motion the stimulus contained driving the other pools. The variance of each pool's output scaled linearly with its mean. The net sensory evidence for each direction, calculated as the difference between one pool's activity and the average activity of the other two, was then fed into an integrator, one for each possible choice. Whichever integrator reached a constant decision threshold first determined the choice, and the time of crossing the decision threshold the decision time. RT was modeled as the sum of the decision time and a fixed residual time, capturing the time needed for aspects of the task other than the decision itself, e.g., initiating an eye movement for reporting the choice. The structure of the model is shown in Figure 2. Further details can be found in Materials and Methods.

If adding the secondary task of reporting a second guess did not alter the way subjects made their primary choice, the same model should still be able to capture the primary choice data and associated RTs from this experiment. To test this, we fitted the model (5 free parameters) to the mean RT data. The result of this fit is shown in Figure 3. Filled circles represent the data (with 95% confidence intervals,

calculated according to the method proposed by Goodman, 1965), lines the model. The motion strength of the strongest motion component in the stimulus is plotted on the horizontal axis, the color of symbols/lines reflects the strength of the other two motion components. The model clearly captures the structure of the mean RT data. If the model were perfect, at least 95% of the evaluated model mean RTs would be expected to be within the 95% confidence intervals associated with the data. Our model is close to that: 13 of the 15 mean RTs (87%) are inside, the two that are outside are still close to the confidence intervals. The estimated model parameters are summarized in Table 2.

To further test whether the model can explain the primary choice data, we compared the model's prediction for the distribution of primary choices with the actual distribution from the experiment (Figure 4). These data have not been used yet, because the model had only been fitted to mean RT data. The plotting conventions are similar to Figure 3. Circles indicate correct choices, squares choices of the direction that had intermediate support, and diamonds choices of the direction that had the weakest support. A perfect model would predict probabilities, at least 95% of which would be expected to be within the 95% confidence intervals associated with the data. While our model is not perfect, 18 of the 23 probabilities (78%) are inside, the five that are outside are still close to the confidence intervals. The good agreement between data and model predictions indicates that the model introduced in Niwa and Ditterich (2008) is still able to explain the primary choice data and associated RTs from the current experiment. Thus, asking subjects to report a second guess apparently did not alter the structure of the decision process.

The same computational model can also explain second guesses

We have demonstrated earlier that subjects can produce informed second guesses when making perceptual decisions between multiple alternatives, but can we gain insight into what governs these

second guesses? The idea behind the highly successful integration-to-threshold models in perceptual decision-making is that decisionmakers accumulate sensory evidence for each of the possible choices until the accumulated evidence for one of them exceeds a decision threshold. How could a subject make an informed second guess in this framework? Assume the decisionmaker had access to the states of the integrators that did not win the race at the time of the threshold-crossing. What should the distribution of second guesses look like if subjects reported the integrator with the overall second-highest accumulated evidence as their second guess, or, equivalently, the option with the larger accumulated evidence out of the two remaining ones? We took the model, which had been fitted to the mean RTs associated with the primary choice and was able to explain the distribution of primary choices, and obtained the expected distributions of second guesses based on the overall second-highest accumulated evidence.

A comparison between the predicted distributions of second guesses and the actual data on correct trials is shown in Figure 5. Symbols again represent the data (and 95% confidence intervals), lines reflect the model predictions. On correct trials, by definition, subjects have already reported the correct option as their primary choice. The correct option is therefore no longer available as a second guess. The relative frequency of reporting the correct option as the second guess (filled circles) has to be zero. The only interesting cases are those where the two weaker motion components had different motion strengths (purple and cyan). Squares indicate how often subjects reported the direction with the intermediate motion strength as their second guess, diamonds how often the weakest motion component was reported.

The same comparison, but now for error trials, is shown in Figure 6. In this case, the correct option can be reported as the second guess, and we had already seen earlier that, across experimental conditions, it was chosen more frequently than chance. The figure shows this relative frequency broken down by experimental condition (circles), adds the relative frequencies of reporting each incorrect option as the

second guess (squares and diamonds), and provides the model predictions for comparison. Why, in contrast to the plots we had seen so far, are the squares below the diamonds in this figure? When reporting their primary choice, subjects were more likely to make an error in favor of the motion component with intermediate support rather than picking the weakest component (see squares and diamonds in Figure 4). The weakest component (diamonds) was therefore available as an option for the second guess in substantially more error trials than the component with the intermediate support (squares), which explains why it was overall chosen more frequently. And why does the probability of reporting the direction of the strongest motion component (blue circles/line) not keep increasing monotonically as a function of motion strength? To make an error in a trial with only a single motion component with 40% coherence in the first place, the accumulated evidence for this direction has to be unusually low. As a consequence, since the second guess is based on the same accumulated evidence, there is also not a sufficient amount of evidence to support choosing this direction as the second guess. A perfect model would again predict probabilities, at least 95% of which would be expected to be within the 95% confidence intervals associated with the data. Across both correct and error trials and not counting the zero-probability events, 26 of the 31 predicted probabilities (84%) are inside, the five that are outside are still pretty close to the confidence intervals. Thus, there is good agreement between the data and model predictions, indicating that the reported second guesses are consistent with the idea that the decisionmaker has access to information about how much sensory evidence had been accumulated for competing unchosen options at the time when sufficient evidence had been collected to commit to a primary choice.

In summary, a computational model with only five free parameters can account for 15 mean RTs, 16 relative frequencies for the primary choice (not counting the 7 trivial cases of uniform choice distributions when all motion components are equally strong and the relative frequency of choosing the third option having to be one minus the sum of the relative frequencies of choosing the first or the

second option), and 18 relative frequencies for the second guess, again excluding the trivial cases. This strongly suggests that the primary choice and the second guess are produced by a common integration-to-threshold decision process.

Second guesses are best explained by the states of the integrators shortly after threshold crossing

While the motion stimulus disappeared from the screen when the saccade for reporting the primary choice was detected, there is a delay between the decision threshold crossing and the saccade onset, and some stimulus information is also still in the visual cortical processing pipeline. In the decision confidence literature, it has been proposed that the decision confidence, which is usually reported after the choice, could be informed by sensory evidence that is processed after the choice has been made (Pleskac and Busemeyer, 2010; Moran et al., 2015). To determine whether additional sensory evidence might have contributed to the reported second guesses in our experiment, we created a variant of the model, where the evidence accumulation was allowed to continue for a fixed period of time after the decision threshold had been crossed, before the non-winning integrators were read out to determine the second choice. Figure 7A shows the deviation between predicted and observed second guesses as a function of the additional integration time. Since the calculated points (blue circles) are simulation-based and therefore slightly noisy, we added a robust polynomial interpolation (solid black line). The best match between predicted and observed second guesses (discrepancy of 0.027) is obtained for an additional integration time of 40 ms (dashed vertical line), i.e., when the integrators are read out shortly after the threshold crossing. The discrepancy clearly increases for longer additional integration times. Thus, the second guesses seem to be affected by a small amount of sensory evidence that is processed after the primary choice has been determined, but still largely rely on the same information, as typical decision times in our experiment are an order of magnitude larger. The predicted relative frequencies of

second guesses for a model with 40 ms of additional integration time are shown in Figures 7B and C. There is no major qualitative difference between these plots and Figures 5 and 6, the match between model predictions (lines) and data (symbols) is just slightly better.

A model waiting for the same decision process to cross a second threshold can be ruled out

To determine whether the second guesses could also be explained by alternative mechanisms that do not require reading out and comparing the accumulated evidence for the options that did not win the race to threshold, we considered several alternative models. First, we evaluated the possibility that the decision process could continue after the first threshold crossing until a second (different) threshold is crossed. The first threshold crossing would determine the primary choice, the second threshold crossing the second choice and the decision time. One can imagine that in situations where there is much stronger evidence for one particular choice compared to the other alternatives, such a second threshold crossing is unlikely to occur within a reasonable amount of time, in particular when the integration is perfect, and the decision bounds are fixed. We therefore also considered mechanisms with leaky integration and collapsing decision bounds (Ditterich, 2006). It turns out, however, that this class of models, even in the presence of leaky integration and collapsing bounds, makes one key qualitative prediction: decision times should increase, rather than decrease, when the evidence gets stronger. As a consequence, the best mean RT fit that can be obtained is largely flat as a function of motion strength, and the remaining error is about 6 times as large as the one for the fit shown in Fig. 3. Figure 8A shows this fitting attempt. This class of models can therefore be ruled out as an alternative explanation.

A model based on a second integration-to-threshold process for determining the second choice makes less accurate predictions for the distribution of second guesses

We also considered the possibility that, as soon as the first threshold crossing occurs, a new decision process, only as a 2AFC between the two remaining options, is started. A threshold crossing of the second decision process would then determine the second choice and the decision time. When enforcing the same decision threshold as in the primary decision process, the remaining error after the mean RT fit is more than an order of magnitude larger than the one for the fit shown in Fig. 3. We therefore considered the possibility that the decision threshold for the second decision process could be lower. The mean RT fit reveals that the threshold would have to be very close to zero to be able to account for the pattern of RTs. A fit with a decision threshold of 0.052 (compared to 1 in the case of the first decision process) resulted in a remaining error that was only slightly larger than the one for the fit shown in Fig. 3. We therefore determined the predicted second guesses for this model (shown in Figure 8B and C). The discrepancy between predicted and observed second guesses, following the same convention as the one used in Fig. 7A, was 0.129 (red dashed line in Fig. 8D), about five times as big as the one for the model shown in Fig. 7B and C. Thus, this model also cannot capture the data pattern as well as our original model.

A model based on a second, fixed-duration decision process for determining the second choice provides the second-best explanation for the distribution of second guesses

As a final possibility, we considered that the second decision process might not be terminated by a threshold crossing, but rather end after a fixed amount of time. The process would be read out at that point, and the sign of the accumulated evidence would determine the second choice. The discrepancy between predicted and observed second guesses for this model, as a function of the duration of the

second decision process, is shown in Figure 8D. Since the calculated points (blue circles) are simulation-based and therefore slightly noisy, we again added a robust polynomial interpolation (solid blue line). The best match is observed for an integration time of 70 ms, but the discrepancy is still 0.081, about three times as big as the one for the model shown in Fig. 7B and C (solid black in Fig. 8D). This model's predictions for the second guesses are shown in Figures 8E and F. In contrast to our original model, which predicted the nonmonotonic relationship between motion strength and the probability of choosing the strongest motion component as the second guess on error trials (blue circles in Fig. 8F), this model predicts a monotonic relationship (blue line). This difference results from the fresh start of evidence accumulation in the second decision process, rather than the second guess being substantially affected by the accumulated evidence that led to the primary choice. Since 70 ms are needed for the second integration process, the residual time would be reduced to 593 ms in this case. While this model provides the second-best explanation, our original model still provides the better explanation for the observed pattern of second guesses.

DISCUSSION

We asked human subjects to make a perceptual decision among three alternatives and to report not only their primary choice, but also a second guess. Our data indicate that this second guess is not random, but clearly informed by the sensory evidence. A single integration-to-threshold model can not only explain the distribution of primary choices and the associated RTs, but also the distribution of second guesses. This suggests that the second guess is generated based on largely the same accumulated evidence that is also used to produce the primary choice. The second guess appears to be governed by the ranking of the amounts of evidence that have been accumulated by the integrators that did not win the race to threshold, which are apparently accessible.

We also considered alternative models. The only other model that was able to largely capture the data pattern, although not as well as the model based on reading out the states of the integrators that had not crossed the decision threshold yet shortly after the winning integrator crossing its threshold, was a model based on starting a new decision process when the threshold crossing determining the primary choice occurred. The process had to be set up as a decision between the remaining alternatives and read out after a fixed amount of time (about 70 ms).

Relationship with decision confidence

Human subjects can not only report their choice when making a perceptual decision, but also express a level of confidence in their decision. A substantial body of literature has been devoted to how well calibrated this decision confidence is and how it might be computed. Ideally, the level of confidence should match the accuracy of the decision. However, this is typically not the case, and human subjects have been reported to be either under- or overconfident, depending on the difficulty of the decision (see Rahnev and Denison, 2018 for a review). Confidence clearly is informed by the available sensory evidence, but how? Vickers (1979) suggested that it depends on the balance of evidence. The more dissimilar the amounts of evidence in favor of the available options are at the time of making a decision, the more confident the observer can be about the choice. This information can be extracted from the decision process itself. While the idea is incompatible with the popular 1-dimensional drift-diffusion model for 2-alternative forced choices, which is equivalent to a race between two accumulators that receive perfectly anti-correlated instantaneous net evidence and, as a consequence, always has the losing integrator in an identical state when the winning integrator exceeds the decision threshold, it can be applied to alternative models. For example, Ditterich (2006) demonstrated that a model based on partially anti-correlated accumulators provides a better account of decision-related activity in the

parietal association cortex of monkeys performing a perceptual decision task. Neurons coding for the losing alternative do not show a stereotyped activity level when the neurons coding for the winning alternative reach threshold. This information could be used to inform confidence. Moreno-Bote (2010) formalized how confidence can be extracted from diffusion models with partially correlated integrators. An alternative mechanism was proposed by Smith and Vickers (1988). According to their model, only one of the integrators is updated at a particular time, the one receiving positive instantaneous net sensory evidence, which also results in the losing accumulator being in different states when the winning accumulator reaches threshold.

Gaining neurophysiological insights into the neural mechanism underlying decision confidence from animal experiments is challenging, as animals cannot be asked directly to provide an explicit confidence rating. However, animal tasks have been developed, which require the animal to produce a behavior that should be informed by decision confidence (see Hanks and Summerfield, 2017 for a review). For example, Kiani and Shadlen (2009) trained monkeys to make a perceptual decision between two alternatives. In a random subset of trials, the researchers offered a third option, a sure bet resulting in a smaller, but certain reward, whereas the animals could gain a larger reward if they engaged in a choice and reported the correct option. The animals were more likely to choose the sure bet the weaker the sensory evidence (motion coherence) was and the shorter they were allowed to watch the motion stimulus. Importantly, decision-related neurons in parietal association cortex that have the signature of carrying accumulated evidence showed either strong or weak activation when the animal engaged in a choice, but intermediate activation when opting for the sure bet, suggesting that the information encoded in these neurons does not only govern choice, but also inform confidence. The study further suggested that decision confidence does not only depend on accumulated evidence, but also on elapsed time, which was confirmed explicitly in a later human psychophysics experiment (Kiani et al., 2014) and is also formalized in Moreno-Bote's (2010) model. Animal experiments on decision confidence have

received some criticism, primarily claiming that the tasks could potentially be solved without requiring any meta-cognition, for example, by treating tasks with a sure bet as a multi-alternative decision task (Insabato et al., 2016, 2017). However, Kepecs and Mainen (2012) pointed out that the same scrutiny should then also be applied to human tasks.

The view that confidence is governed by the same information that determines the choice and, in particular, by the balance of evidence has been challenged by experiments that found that confidence primarily relies on response-congruent evidence (Zylberberg et al., 2012; Maniscalco et al., 2016). The authors reported that, while choices in their experiments were governed by the balance of evidence, confidence was primarily determined by the amount of evidence for the chosen option and largely insensitive to the amount of evidence for the non-chosen alternative. Dual stage or second-order models are also at odds with the idea that choice and confidence rely on the same information (Pleskac and Busemeyer, 2010; Moran et al., 2015; Fleming and Daw, 2017). These models posit that confidence ratings rely on a post-decision process that is informed by the outcome of the decision process, but not exclusively.

Different studies have therefore found the information upon which choice and decision confidence are based to overlap to varying degrees. We have addressed a similar question for the mechanism underlying second guesses. Our results indicate that the distribution of second guesses is most compatible with a decision mechanism that largely uses the same accumulated evidence for determining both the primary and the second choice. We found the best match between model predictions and data, when the decision process was allowed to continue for a very short period of time (compared to typical decision times in our experiment), about 40 ms, after the threshold crossing determining the primary choice, before the states of the remaining integrators are read out to determine the second choice.

559

560 *Second guessing in other cognitive functions*

561 In 1961, Signal Detection Theory (SDT) was still in its infancy and competing with the prevailing "high
562 threshold" model of sensory perception, Swets and colleagues published a paper proposing that a
563 second-choice paradigm in multi-interval signal detection could help distinguishing between the
564 competing ideas (Swets et al., 1961). However, second-choice paradigms have not been pursued further
565 in the area of perceptual decision-making, in particular not since the field has turned to sequential
566 sampling models to explain not only choices, but also decision times. Instead, Swets et al.'s proposal got
567 picked up in the memory literature, there typically referred to as a 4AFC-2R (four-alternative forced
568 choice with two responses) paradigm, as the field was also debating whether recognition memory was
569 best described by a threshold process or by a continuous memory strength process. Parks and
570 Yonelinas (2009) used a second-choice paradigm to gather experimental evidence beyond the Receiver
571 Operating Characteristic analysis that the field had relied on previously. Kellen and Klauer (2011)
572 followed up with a more detailed model-based analysis. Earlier, second guesses had already been used
573 to study mechanisms underlying the effect of misinformation on memory recall (Wright et al., 1996).
574 More recently, second guesses have also been used to study conflict detection mechanisms in reasoning
575 (Bago et al., 2019).

576

577 *Second guesses as a tool for studying knowledge about the decision process*

578 We have shown that human subjects can produce informed second guesses when making perceptual
579 decisions between multiple alternatives and that these second choices follow a distribution that would
580 be expected if they were governed by the relative amounts of accumulated net sensory evidence for
581 each option at the time of the largest accumulated evidence reaching a bound. Second-choice

paradigms therefore cannot only be used in the context of SDT, as they have in the past, but also with accumulation-of-evidence frameworks. In addition to decision confidence, the study of second guesses provides another useful tool for gaining insight into the decision process and what information a decisionmaker has access to about the outcome of a decision, beyond the discrete choice. Similar to the neurophysiological work on decision confidence, we expect future studies to be able to establish a link between second guesses and underlying neural activity.

REFERENCES

Bago B, Raoelison M, De Neys W (2019) Second-guess: Testing the specificity of error detection in the bat-and-ball problem. Acta Psychol (Amst) 193:214-228.

Bollimunta A, Totten D, Ditterich J (2012) Neural dynamics of choice: single-trial analysis of decision-related activity in parietal cortex. J Neurosci 32:12684-12701.

Brainard DH (1997) The Psychophysics Toolbox. Spat Vis 10:433-436.

Ditterich J (2006) Stochastic models of decisions about motion direction: behavior and physiology. Neural Netw 19:981-1012.

Ditterich J (2010) A Comparison between Mechanisms of Multi-Alternative Perceptual Decision Making: Ability to Explain Human Behavior, Predictions for Neurophysiology, and Relationship with Decision Theory. Front Neurosci 4:184.

Fleming SM, Daw ND (2017) Self-evaluation of decision-making: A general Bayesian framework for metacognitive computation. Psychol Rev 124:91-114.

Forstmann BU, Ratcliff R, Wagenmakers EJ (2016) Sequential Sampling Models in Cognitive Neuroscience: Advantages, Applications, and Extensions. Annu Rev Psychol 67:641-666.

Goodman LA (1965) On Simultaneous Confidence Intervals for Multinomial Proportions. Technometrics 7:247-254.

Hanks TD, Summerfield C (2017) Perceptual Decision Making in Rodents, Monkeys, and Humans. Neuron 93:15-31.

Insabato A, Pannunzi M, Deco G (2016) Neural correlates of metacognition: A critical perspective on current tasks. Neurosci Biobehav Rev 71:167-175.

Insabato A, Pannunzi M, Deco G (2017) Multiple Choice Neurodynamical Model of the Uncertain Option Task. PLoS Comput Biol 13:e1005250.

Kellen D, Klauer KC (2011) Evaluating models of recognition memory using first- and second-choice responses. J Math Psychol 55:251-266.

Kepecs A, Mainen ZF (2012) A computational framework for the study of confidence in humans and animals. Philos Trans R Soc Lond B Biol Sci 367:1322-1337.

Kiani R, Shadlen MN (2009) Representation of confidence associated with a decision by neurons in the parietal cortex. Science 324:759-764.

Kiani R, Corthell L, Shadlen MN (2014) Choice certainty is informed by both evidence and decision time. Neuron 84:1329-1342.

Latimer KW, Yates JL, Meister ML, Huk AC, Pillow JW (2015) Single-trial spike trains in parietal cortex reveal discrete steps during decision-making. Science 349:184-187.

Luce RD (1986) Response Times: Their Role in Inferring Elementary Mental Organization: Oxford University Press.

Maniscalco B, Peters MA, Lau H (2016) Heuristic use of perceptual evidence leads to dissociation between performance and metacognitive sensitivity. Atten Percept Psychophys 78:923-937.

Moran R, Teodorescu AR, Usher M (2015) Post choice information integration as a causal determinant of confidence: Novel data and a computational account. Cogn Psychol 78:99-147.

628 Moreno-Bote R (2010) Decision confidence and uncertainty in diffusion models with partially correlated
629 neuronal integrators. Neural Comput 22:1786-1811.
630 Niwa M, Ditterich J (2008) Perceptual decisions between multiple directions of visual motion. J Neurosci
631 28:4435-4445.
632 Palmer J, Huk AC, Shadlen MN (2005) The effect of stimulus strength on the speed and accuracy of a
633 perceptual decision. J Vis 5:376-404.
634 Parks CM, Yonelinas AP (2009) Evidence for a memory threshold in second-choice recognition memory
635 responses. Proc Natl Acad Sci U S A 106:11515-11519.
636 Pelli DG (1997) The VideoToolbox software for visual psychophysics: transforming numbers into movies.
637 Spat Vis 10:437-442.
638 Pleskac TJ, Busemeyer JR (2010) Two-stage dynamic signal detection: a theory of choice, decision time,
639 and confidence. Psychol Rev 117:864-901.
640 Rahnev D, Denison RN (2018) Suboptimality in Perceptual Decision Making. Behav Brain Sci:1-107.
641 Ratcliff R, Smith PL (2004) A comparison of sequential sampling models for two-choice reaction time.
642 Psychol Rev 111:333-367.
643 Ratcliff R, McKoon G (2008) The diffusion decision model: theory and data for two-choice decision tasks.
644 Neural Comput 20:873-922.
645 Roitman JD, Shadlen MN (2002) Response of neurons in the lateral intraparietal area during a combined
646 visual discrimination reaction time task. J Neurosci 22:9475-9489.
647 Shadlen MN, Newsome WT (2001) Neural basis of a perceptual decision in the parietal cortex (area LIP)
648 of the rhesus monkey. J Neurophysiol 86:1916-1936.
649 Smith PL, Vickers D (1988) The Accumulator Model of 2-Choice Discrimination. J Math Psychol 32:135-
650 168.
651 Swets J, Tanner WP, Jr., Birdsall TG (1961) Decision processes in perception. Psychol Rev 68:301-340.

652 Treue S, Hol K, Rauber HJ (2000) Seeing multiple directions of motion-physiology and psychophysics. Nat
653 Neurosci 3:270-276.
654 Vickers D (1979) Decision Processes in Visual Perception: Academic Press.
655 Wright DB, Varley S, Belton A (1996) Accurate second guesses in misinformation studies. Appl Cognitive
656 Psych 10:13-21.
657 Zylberberg A, Barttfeld P, Sigman M (2012) The construction of confidence in a perceptual decision.
658 Front Integr Neurosci 6:79.

659

660 **Table 1. List of motion coherence combinations**

Motion coherence of first component [%]	Motion coherence of second component [%]	Motion coherence of third component [%]
0	0	0
5	0	0
0	5	0
0	0	5
10	0	0
0	10	0
0	0	10
20	0	0
0	20	0
0	0	20
40	0	0
0	40	0
0	0	40
10	10	10
20	10	10
10	20	10
10	10	20
30	10	10
10	30	10
10	10	30

20	15	5
20	5	15
15	20	5
5	20	15
15	5	20
5	15	20
30	15	5
30	5	15
15	30	5
5	30	15
15	5	30
5	15	30
20	20	20
30	20	20
20	30	20
20	20	30
40	20	20
20	40	20
20	20	40
30	25	15
30	15	25
25	30	15
15	30	25

25	15	30
15	25	30
40	25	15
40	15	25
25	40	15
15	40	25
25	15	40
15	25	40

661

662

663 **Table 2. Best-fitting model parameters**

Model parameters	Parameter values
g	0.0103
k_n	0.197
k_s	0.616
k_v	0.329
Residual time (ms)	663

664

665

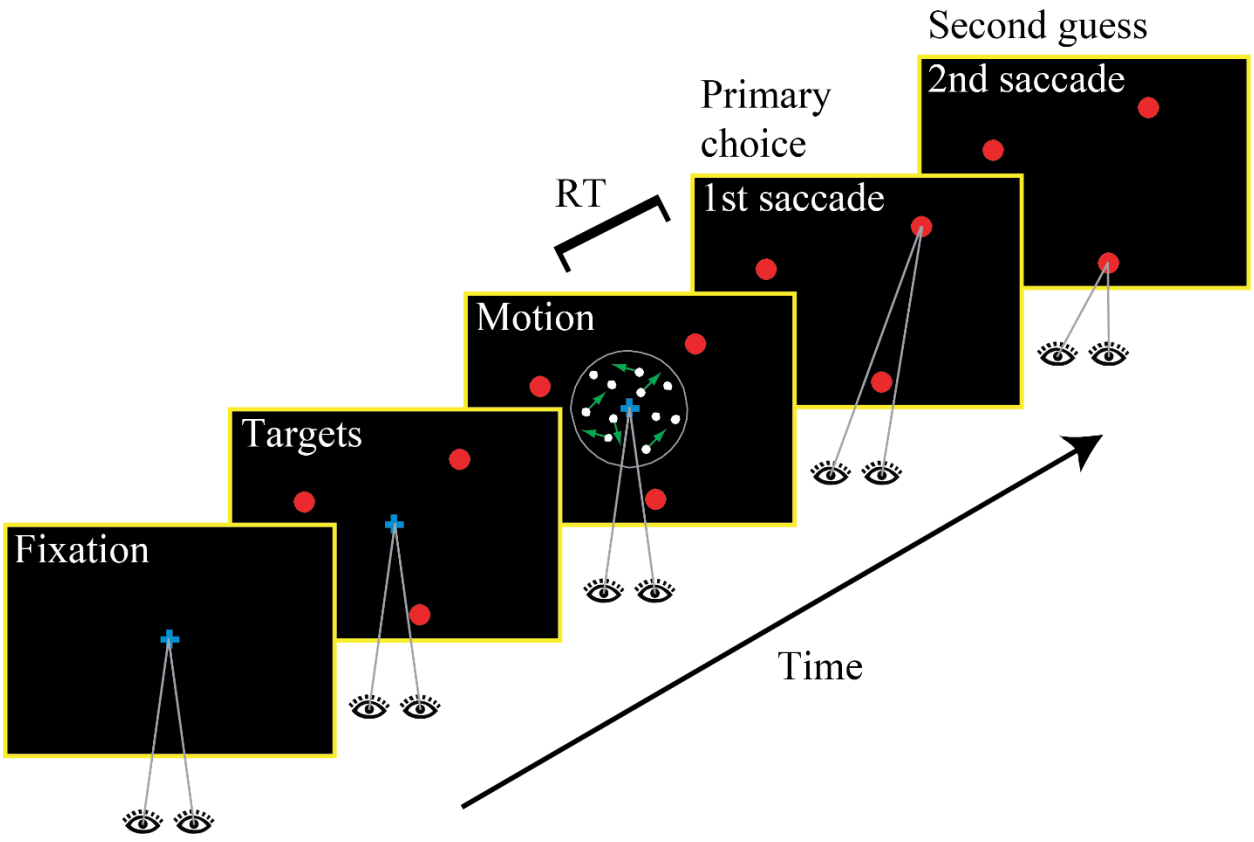

Figure 1. Experimental paradigm. Human subjects were asked to determine the strongest motion direction in a random-dot pattern with multiple motion components. They were free to watch the stimulus as long as they wanted and responded with a goal-directed eye movement to one of three choice targets to indicate their primary choice. Choices and RTs were measured. After indicating their primary choice, subjects were instructed to make a second goal-directed eye movement to one of the remaining two targets to indicate a second guess.

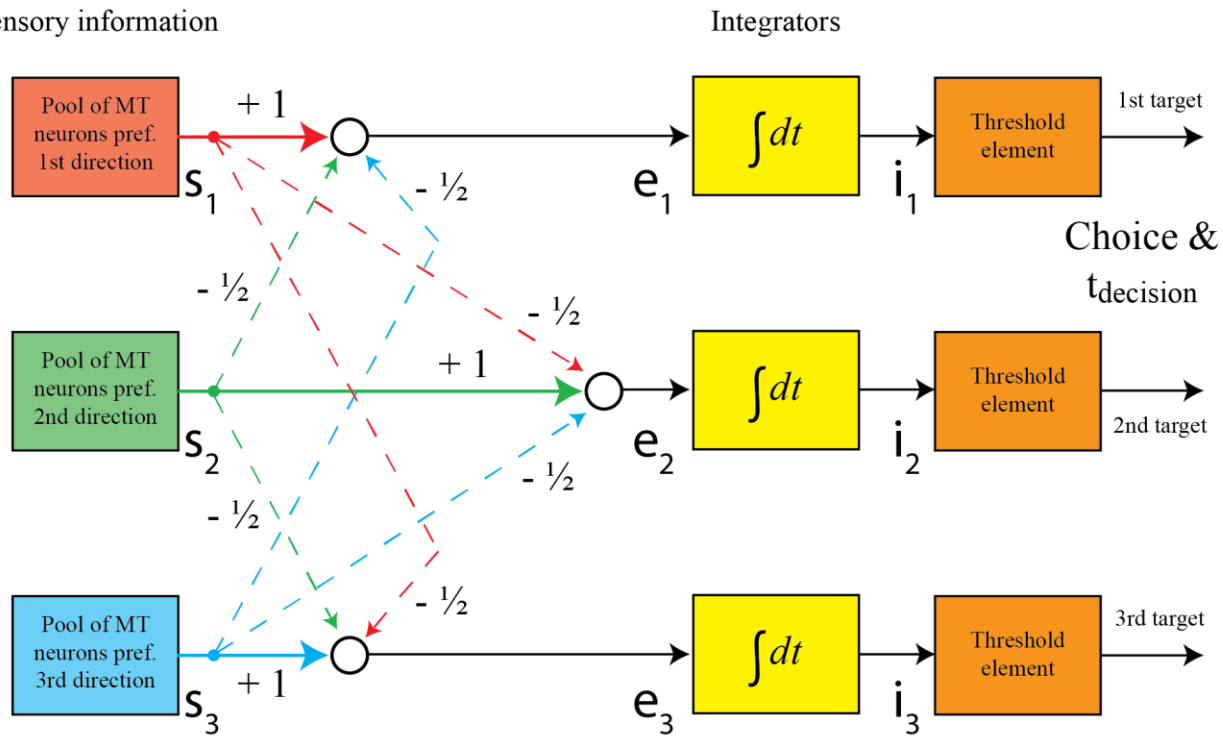

675

676

677 **Figure 2.** Computational model. Three integrators (each associated with one of the three alternatives)

678 race against each other. The integrator output signal (i_1 , i_2 , or i_3) reaching a decision threshold first

679 determines the primary choice and terminates the decision process. The integrator input signals (e_1 , e_2 ,

680 and e_3) are net evidence signals, which are linear combinations of the three relevant sensory signals

681 (s_1 , s_2 , and s_3). Solid arrows indicate positive weights (excitatory connections), and dashed arrows

682 indicate negative weights (inhibitory connections). The second guess is determined by the rank ordering

683 of the remaining two integrators when the winning one reaches threshold.

684

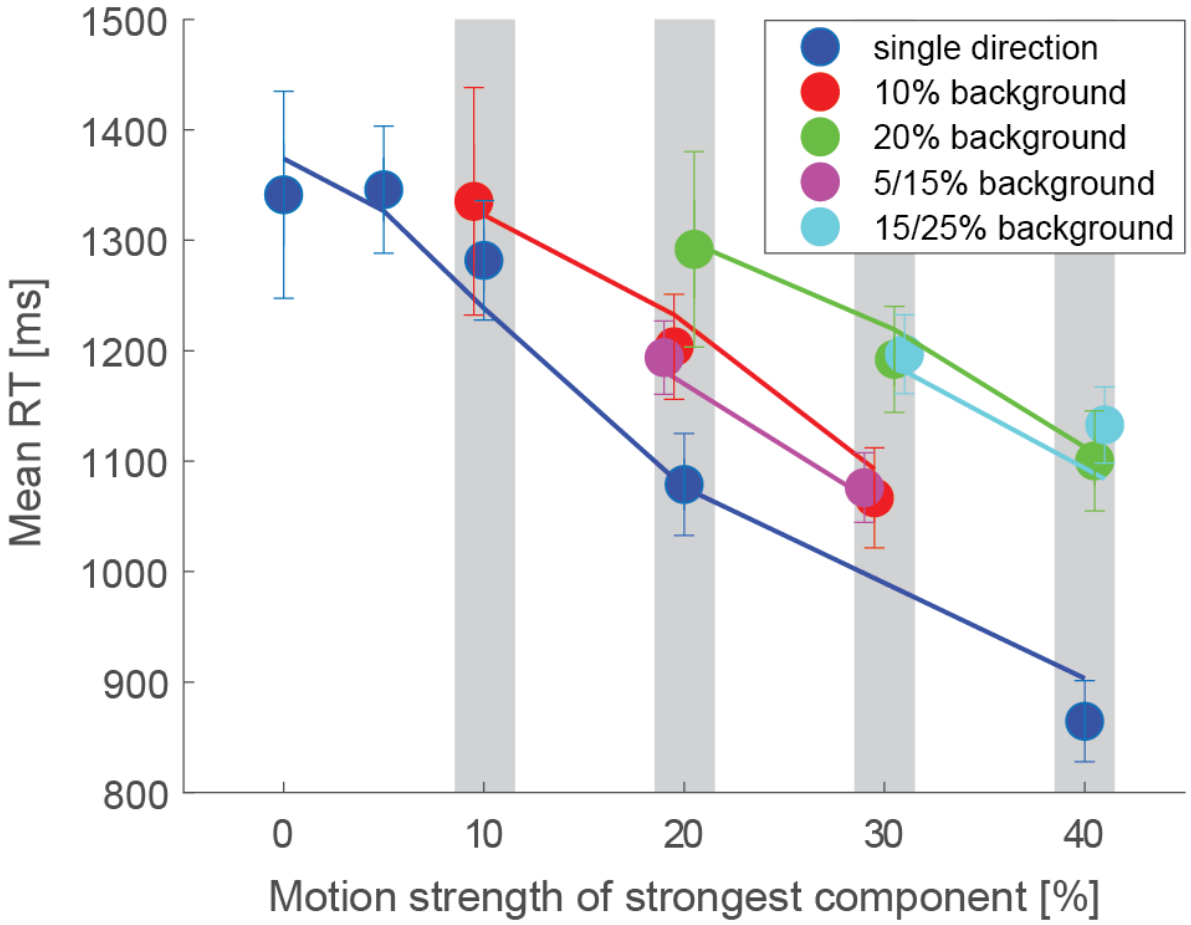

685

686

687 **Figure 3.** Mean response time data and fitted model. The symbols represent the measured mean RTs for
688 all unique combinations of motion strengths. The motion strength of the strongest component is plotted
689 on the horizontal axis. Colors indicate the motion strengths of the two weaker motion components. (For
690 example, the cyan point at 40% motion strength indicates the mean RT for stimuli with the three motion
691 components having strengths of 40%, 25%, and 15%, respectively.) Some points have been shifted
692 slightly horizontally to reduce graphical overlap. For example, all points within the gray bar centered on
693 20% have a strength of the strongest motion component of exactly 20%. Error bars indicate 95%
694 confidence intervals. The lines connect the mean RTs from the computational model.

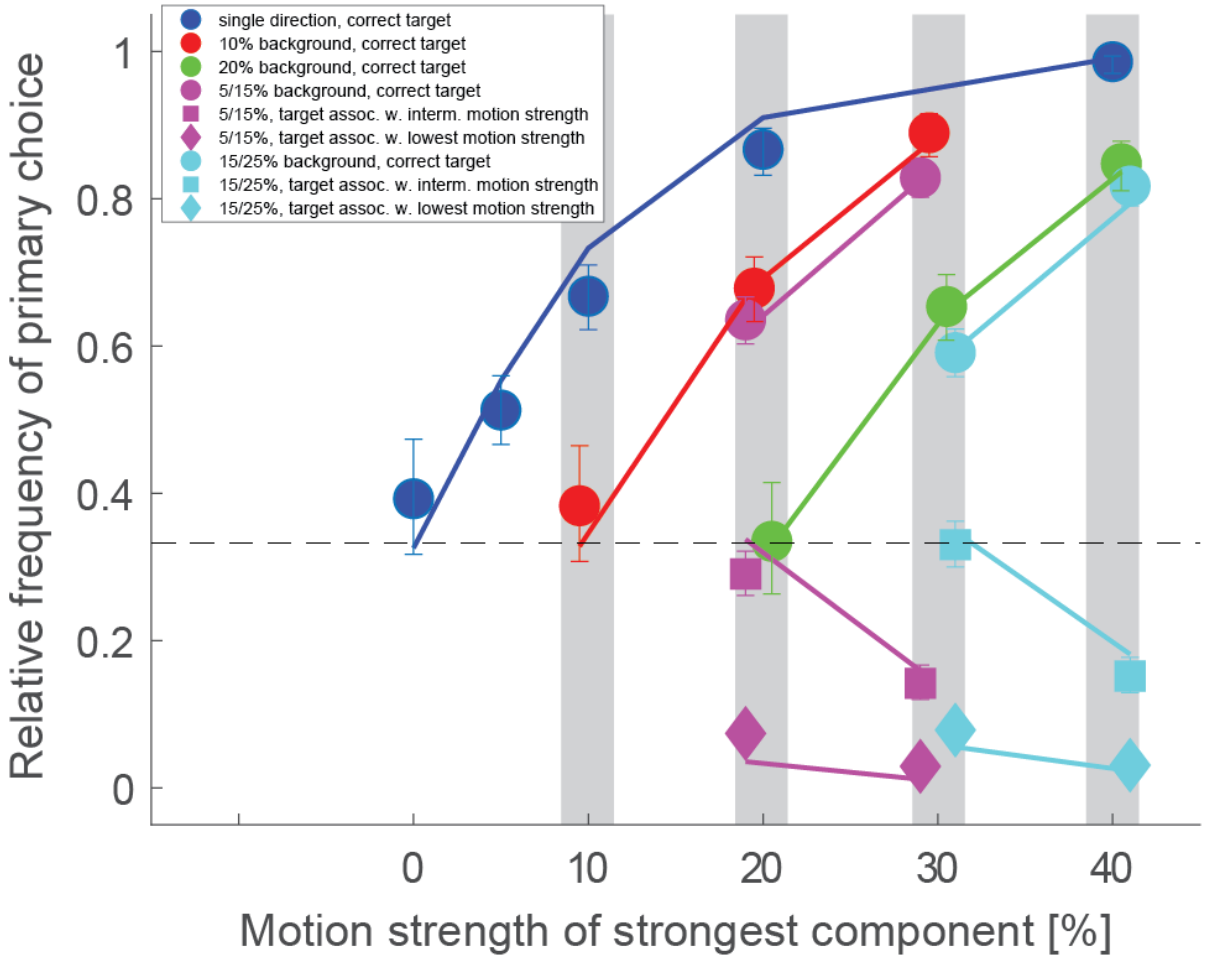

695

696

697 **Figure 4.** Comparison between the relative frequencies of primary choices and model predictions.
698 Symbols again reflect the data, with error bars indicating 95% confidence intervals. The lines connect
699 the relative frequencies predicted by the computational model. Circles indicate choices of the target
700 associated with the strongest motion component (correct primary choices), squares choosing the target
701 associated with the component with intermediate motion strength, and diamonds choosing the target
702 associated with the weakest motion component. Other conventions as in Fig. 3. The dashed line
703 indicates chance performance.

704

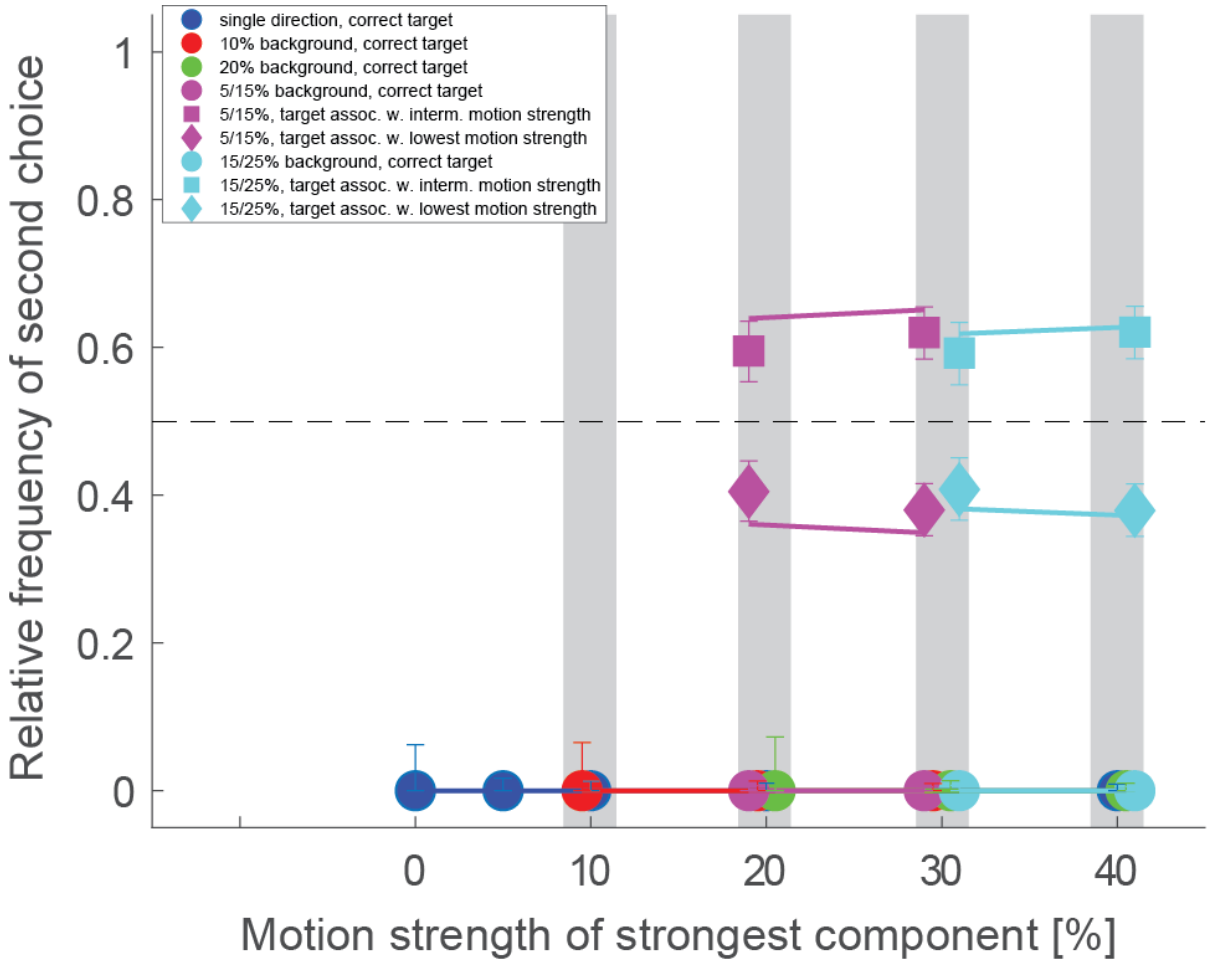

705

706

707 **Figure 5.** Comparison between relative frequencies of second guesses on correct trials (symbols, with

708 error bars indicating 95% confidence intervals) and model predictions (lines). Conventions as in Fig. 4.

709 Note that on correct trials the target associated with the strongest motion component has been

710 reported as the primary choice and is not available for the second guess. Therefore, all circles are

711 located at a relative frequency of zero.

712

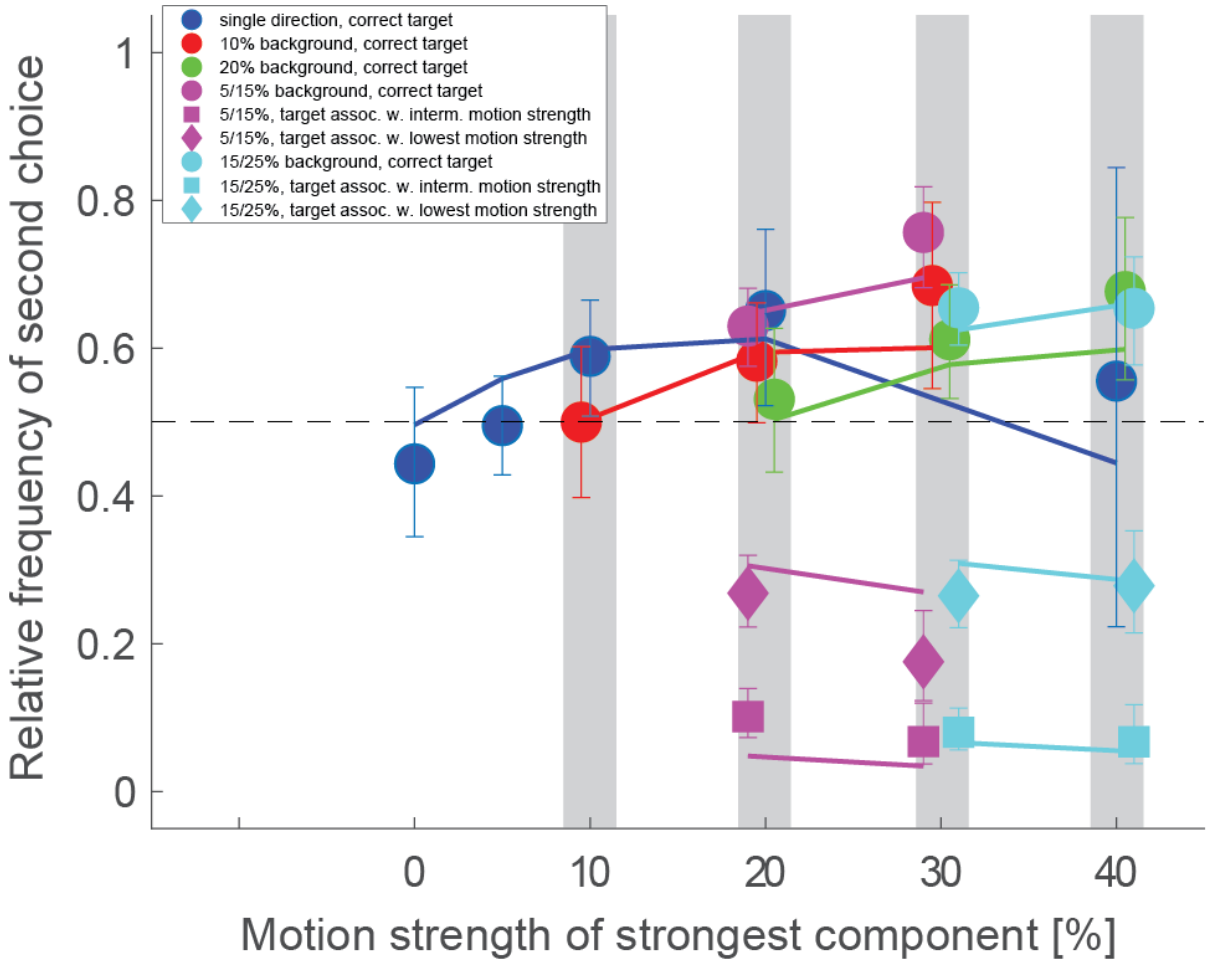

713

714

715 **Figure 6.** Comparison between relative frequencies of second guesses on error trials (symbols, with

716 error bars indicating 95% confidence intervals) and model predictions (lines). Conventions as in Fig. 5.

717 How often the correct target (circles) was reported as the second choice varied across experimental

718 conditions, but was overall significantly above chance (63%).

719

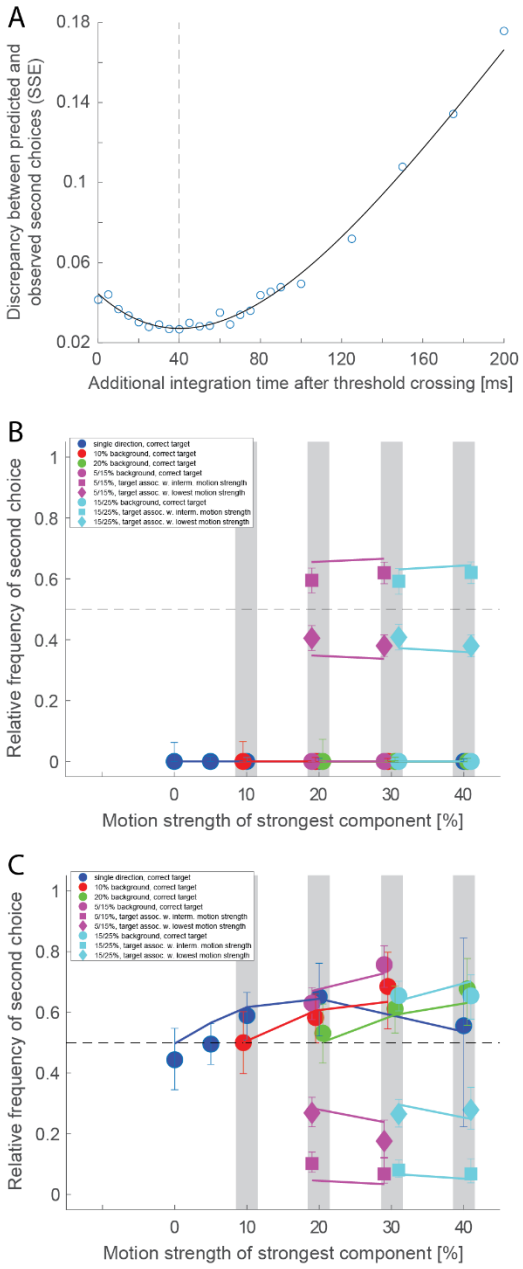

720

721 **Figure 7.** Predictions for second guesses when integration is allowed to continue after the threshold
722 crossing. **A.** Discrepancy between predicted and observed second guesses as a function of additional
723 integration time before the accumulated evidence is read out. A minimum (best match) is observed at
724 40 ms. **B.** Predicted second guesses on correct trials with 40 ms additional integration time (same format
725 as Fig. 5). **C.** Predicted second guesses on error trials with 40 ms additional integration time (same
726 format as Fig. 6).

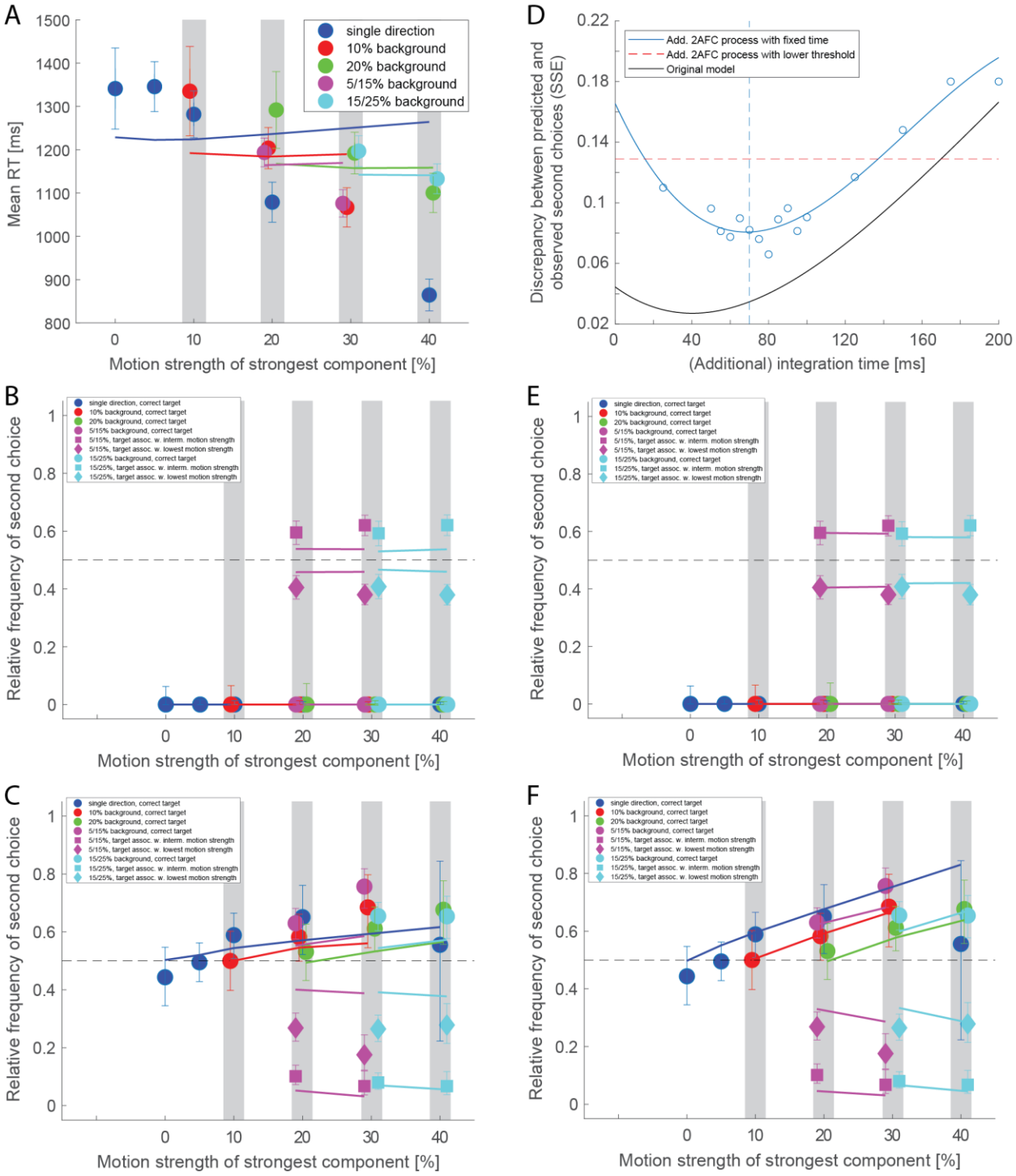

Figure 8. Alternative models. **A.** Mean RT fit for a model that waits for a second threshold crossing, but allowing leaky integration and collapsing bounds (same format as Fig. 3). **B.** Predicted second guesses on correct trials for a model that starts a new 2AFC decision process to determine the second choice and

731 waits for a threshold crossing, but allowing a lower threshold than in the primary decision process (same
732 format as Fig. 5). **C.** Like B, but for error trials (same format as Fig. 6). **D.** Discrepancy between predicted
733 and observed second guesses as a function of integration time for a model that starts a new 2AFC
734 decision process to determine the second choice and reads the process out after a fixed amount of time
735 (blue). A minimum (best match) is observed at 70 ms. For comparison, the curve for the original model
736 (black) and the value for the model with a low threshold (red) are also shown. **E.** Predicted second
737 guesses on correct trials for a model that starts a new 2AFC decision process to determine the second
738 choice and integrates the sensory evidence for 70 ms before the process is read out (same format as
739 Fig. 5). **F.** Like E, but for error trials (same format as Fig. 6).

740